Proceedings of the 28th IEEE
EMBS Annual International Conference
New York City, USA, Aug 30-Sept 3, 2006

Virtual Walls in Microchannels

Wei Xu, Hong Xue, Mark Bachman and G.P. Li

Abstract —**Microfluidic channels were studied, in which the surface is modified from a solid/liquid interface into solid/liquid and air/liquid alternating interface, creating the equivalent of a superhydrophobic surface on the interior of the channel. The composite microchannel can be easily fabricated using embossing or cast molding of PDMS. The channels are stable under typical microfluidic conditions. For the most part, fluid flow behavior is not significantly changed; however, interesting mass transport effects can be observed in such channels under appropriate conditions. An application example of a microvalve based on the mass transport effect is demonstrated, showing advantages of simple design, fabrication, no moving part and zero dead volume.**

I. INTRODUCTION

Surfaces represent a major challenge to the success of microfluidic devices and small volume systems. High surface area to volume ratios at small scales imply that chemical and physical interactions at the surfaces will dominate bulk fluidic phenomena in micromachined systems. To reduce the role of surfaces, substantial research effort has been expended on modifying the surfaces of microchannels. Many approaches have been studied, and can be divided into two categories: chemical approaches[1]-[6] and physical approaches[7]-[12].

In this paper, we present a method to minimize surface interaction by introducing air or oil directly into the wall of a microfluidic channel to reduce fluid contact with the solid material of the channel walls. Since neither the air nor oil are solid, these form a "virtual wall" in microfluidic channel that replaces the solid wall. This method is conceptually identical to the method of generating super-hydrophobic surfaces using micro (or nano) needles on a surface [13][14]. The difference is that in the current work, these super-hydrophobic surfaces are enclosed in a microfluidic device. This type of surface reduces the physical contact between reagent and the solid walls.

A simple 2-D version of the channel is shown in figure 1. A microfluidic device is constructed from polydimethylsiloxane (PDMS) by standard casting methods: liquid PDMS is poured over a silicon micromold, then hardened to produce a polymer microfluidic device. The design of the channel includes a periodic arrangements of micro-cavities that provide dead volumes within the channel. The purpose for these dead volumes is to trap air or oil when sample fluid is introduced in the channel.

We built a number of prototype channels for this study. The dimension of channel discussed here is 150 μm × 50 μm × 4.5 cm ($W \times D \times L$). The dimension of micro-cavities is 80 μm × 70 μm × 50 μm ($W \times H \times D$). The pitch of the micro-cavities is 140 μm. Since the PDMS is naturally hydrophobic, the dead regions trap air when water is introduced into the channel, as shown in Fig. 1b. The surface tension of the water prevents water moving into the cavities as long as the pressure difference applied on the channel is small, which is satisfied in the typical operation of the microfluidic device. The result of air bubbles trapped in the channel is that the walls contain both liquid/solid and liquid/air interfaces, or "virtual walls". We noticed that air bubbles were retained in PDMS channel cavities for many hours, though ultimately, the bubbles would shrink. We believe this is due to the porous nature of PDMS that can absorb gasses into the solid material. Related experiments with SU-8 and glass cavities have shown that these bubble-lined surfaces can be stable for weeks.

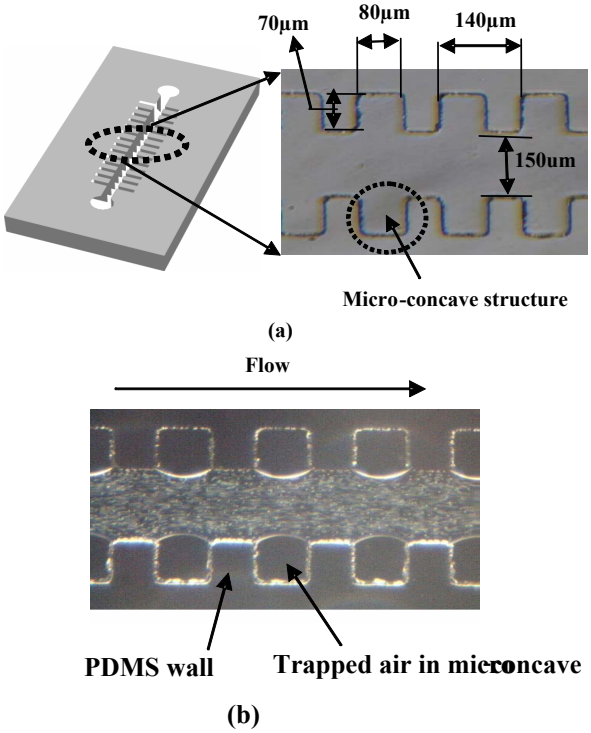

Figure 1: (a) View of microchannels with micro cavities designed to trap air. (b) Image of fluid flow in microchannels with trapped air cavities. Water contains 1 micron polystyrene beads to help visualization. Water in channels is exposed to channel walls and air walls.

II. EXPERIMENTS AND DISCUSSION

To test whether the bubbles were stable under flow

Manuscript received April 3, 2006.

Wei Xu is with the Electrical Engineering and Computer Science and Integrated Nanosystem Research Facility, University of California, Irvine, CA 92697 USA(e-mail:wxu@uci.edu).

Hone Xue is with Mechanical Engineering Department, California State Polytechnic University, Pomona, CA, 91768(e-mail :hxue@csupomona.edu)

Mark Bachman is with the Electrical Engineering and Computer Science, and Integrated Nanosystem Research Facility, University of California, Irvine, CA 92697 USA(e-mail:mbachman@uci.edu).

G.P.Li is with the Electrical Engineering and Computer Science and Integrated Nanosystem Research Facility, University of California, Irvine, CA 92697 USA(e-mail:gpli@uci.edu)

conditions, we performed two separate measurements. One utilized pressure driven flow; the second observed electro-osmotic flow. In both cases, a microfluidic device was constructed that contained two parallel channels. The first channel was a reference channel, with no cavities. The second channel consisted of microcavities (with above dimensions) that were filled with air. The two chambers were joined by a "T" connection at one end, allowing them to share a common fluidic channel.

Pressure flow. Water was injected through the two channels (reference channel and virtual wall channel) simultaneously using reservoirs set to identical heights that connected to the microchannels by small tubing. One water contained a dye as an indicator. The image of the two fluids at the "T" junction exit is shown in Figure 2. The ratio of the two flow rates is reflected in the position of the Laminar flow boundary. The flow rates were nearly identical, which was determined by the location of the Laminar flow boundary. Air bubbles were seen to stay in their cavities for pressure drops ranging from a few centimeters to over 20 cm of water.

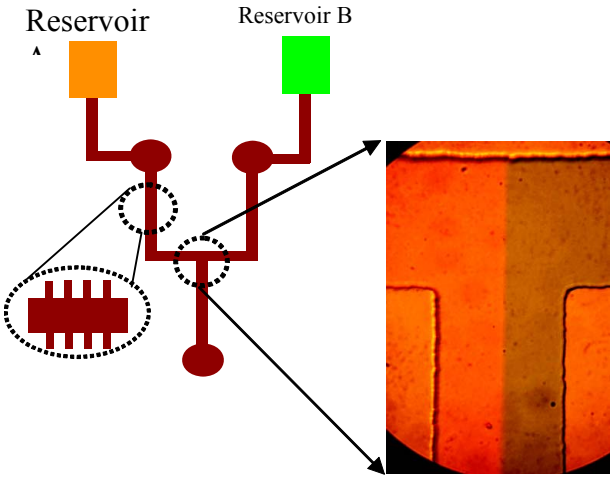

Figure 2: Position of Laminar flow boundary at exit of two joined channels. One channel contained virtual walls, the second had conventional walls.

Electrokinetic flow.and mass transport effect Water was injected through the two channels (reference channel and virtual wall channel) as before. Positive electrodes were inserted to reservoirs A and B, and a ground electrode was placed at the common reservoir. Voltage for electro-osmotic flow was generated by a high voltage module (Ultravolt, model 4A12P4Y5). A microscope (Olympus, BH2-UMA) was used to visualize flows in the composite channel and a digital video camera was mounted on the oculus of the microscope to record the flow. The camera was connected to a PC via USB cable at the same time so that both real-time video and snapshot can be captured by the PC. The buffer prepared for electro-osmotic was 4 mM phosphate buffer with pH = 8. A multi-meter (Wavetek, Model HD110B) was connected between two reservoirs to measure voltage in the channel flow. To visualize flow pattern, 1um polystyrene beads was added into water. Videos of flows in the composite channel were recorded by CCD camera and compared with normal straight channel. At voltage<800V, bubbles remained throughout the experiment and inspection of the video images that were taken reveal no significant difference in the velocity of tracer beads in either the reference of virtual wall channels. However, at higher voltages (>800V), we observed almost immediate random formation of sub-micron water droplets in the air cavities with applied current. These droplets gradually grew to large drops that displaced air into the main section of the micro-fluidic channel, Figure 4.

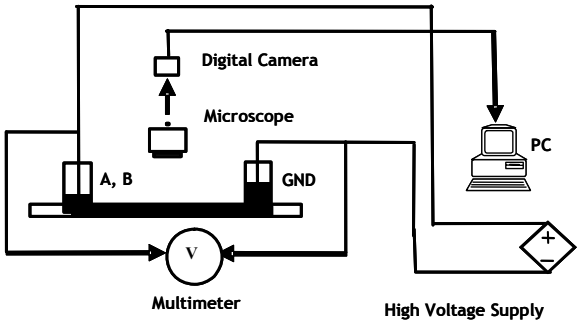

Figure 3: Layout of experiment described in this paper.

With the continuous addition of voltage, the air bubbles further expanded into the channel. Eventually two side wall bubbles touched each other and then coalesced, thus blocked the channel and the flow in virtual wall branch channel was stopped. The above whole process was highly repeatable and approximately took a few minutes. We noticed that the drop growth rate increased with applied voltage. When voltage is greater than 1200V, the bubble could close channels in tens of seconds.

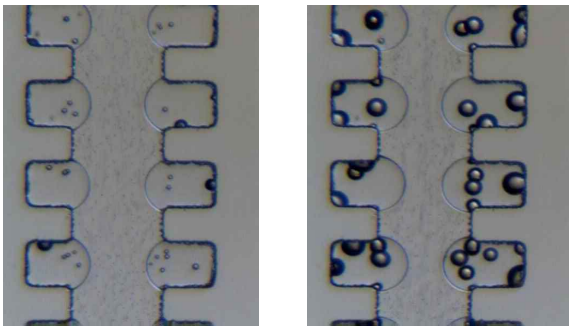

(a) (b)

Figure 4: Condensation occurs in the air-filled cavities in a micro-channel. (a) right after the voltage was added, nanodroplets appeared in the air cavities (b) as the continuous add of voltage, droplets grew to large drops and displaced air into the main section of the channel.

This effect can be explained in terms of mass transport through the vapor phase. At higher voltages, the microchannels experience significant Joule heating, resulting in an increase in temperature of the buffer. Thus water in buffer evaporates into the air-filled cavities, and encounters the cooler PDMS cavities walls which remain at a temperature closeer to room temperature. Warm vapor evaporated from the liquid-vapor interface saturates the small cool cavities, and condensation quickly takes place on the

surfaces of the cavity. As long as the voltage is applied, the buffer is heated and the evaporating and condensing effect continue. Joule heating increases with the input power which is determined by voltage and buffer concentration. The higher the applied voltage or higher buffer concentration, the higher the current and so the higher the temperature of the buffer. The result of this temperature gradient is a mass transfer through the vapor phase from the bulk liquid in the microchannel to the air-filled cavity walls.

Microvalve based on mass transport effect of virtual wall

Devices can be designed based on the above described mass transport effect; we demonstrate a microvalve by example. The design is shown in Figure 5. On one branch of a "T" junction channel, a pair of micro air cavities was fabricated on two side walls of the channel (the microvalve). To prevent the resultant air bubble being flushed downstream by the fluid flow, the channel width after the cavity structures were reduced from w_1=150um to w_2=50um. Instead of using Joule heating, the temperature gradient was created by an external coil heater (nichrome wire) placed underneath PDMS chip and on the upstream of the microvalve. Use of an external heater is more suitable for typical microfluidic applications, and also demonstrates that the mass transport effect is caused by temperature gradient, not electro-kinetic effects.

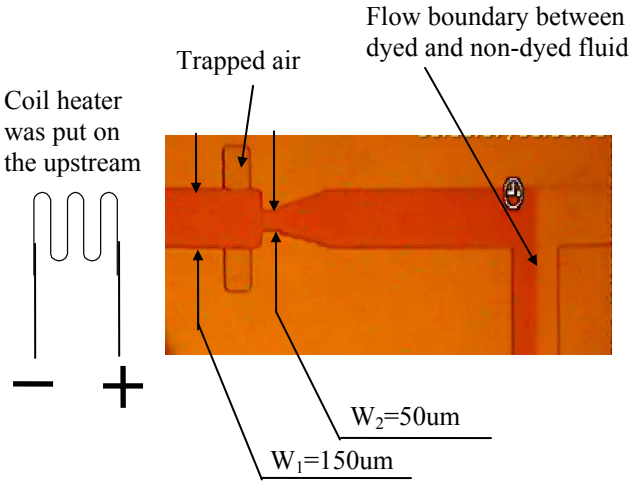

Figure 5: Design of microvalve based on mass transport effect of virtual wall.

During normal operation, the valve is "open" allowing free passage of water into the T-channel (Figure 6). The flows in this microvalve experiment were driven by hydrostatic pressure, which remained at 8 cm water for all experiments. At t<0, the flow rate of the reference channel (not dyed) channels was reduced so that almost all the resulting flow in the common channel came from the dyed side of the device. Then at t=0, the coil heater was turned on, heating the upstream section of the channel before the microvalve. Immediately, the mass transport phenomenon was observed in the cavity structures. Clear droplets formed in the cavities, causing the air bubbles to grow and expand into the main section of the channel. We note that the lack of color in the droplets suggests that the droplets were free of dye, consistent with an evaporation/condensation model of the phenomenon.

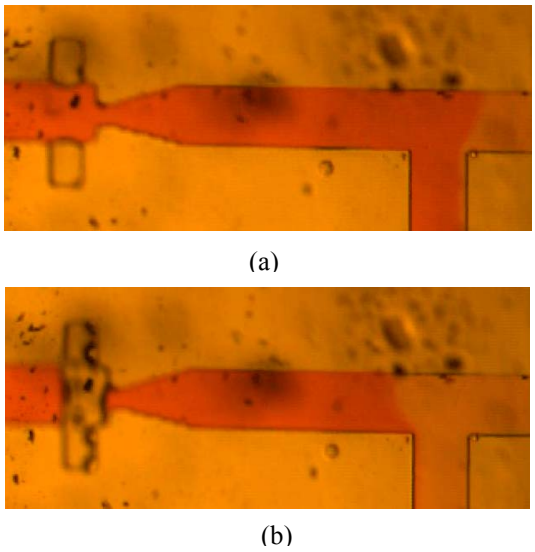

Figure 6: "Open" (a) and "Closed" (b) state of the microvalve. Closed state has air filled chamber.

Eventually two bubbles from the two cavities coalesced and formed a physical air barrier to stop the flow and then heater was turned off. The flow rate of the branch channel with the microvalve was then reduced to zero and then only non-dyed fluid existed in the downstream of T junction. Relative flow rate was determined by monitoring the location of the laminar flow boundary between dyed and non-dyed fluid in the downstream of T junction. Videos of fluid flow were recorded by a NIKON Coolpix 990 mounted on the microscope, then converted into grey scale images and analyzed by a Matlab to calculate pixels intensity value in the T junction region. Aligning these values along the time axis, we determined relative flow rate change during valve operation. This is plotted in Figure 7. The voltage added to the coil heater was 0.8V and the current was 250mA (input power is 200 mW). However, the coil of heater wire was poorly coupled to the microchannel.

Similar to the mass transport experiment in EOF measurement, the droplets growth rate which determined "close" speed of the microvalve increased as the increase of the input power. Four different input powers were tested on the microvalve and were drawn in the Figure 8 vs. response time of the microvalve. It can be seen the response time of the microvalve reduced dramatically from 200s to 25s as the input power increased from 0.056w to 0.31w.

While this study demonstrates the operation of a vapor valve, the input power required for the valving actuation is still too great for typical microscale applications. However, this is almost certainly the result of poor thermal coupling between our test heater and the microfluidic channel. This can be easily remedied by fabricating an integrated microheater on the chip. Furthermore, with the aid of lithographically defined microheaters, multiple vapor valves could be easily

integrated into microfluidic network thus forming a programmable microfluidic valving system.

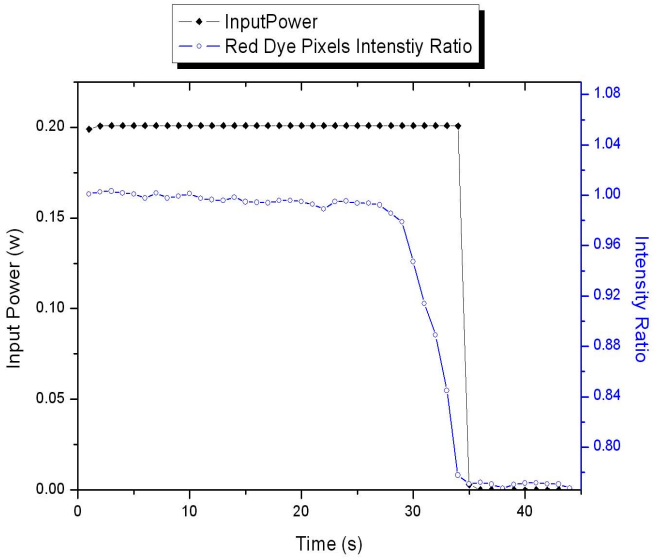

Figure 7: Control signal (input power) and response of the valve (represented by red dye pixels intensity ratio)

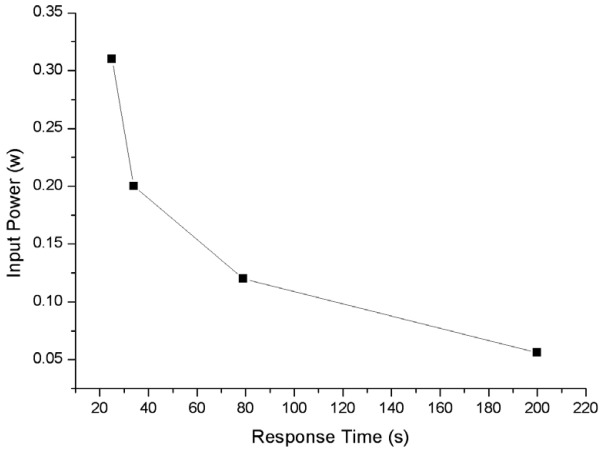

III. CONCLUSION

In this paper we present the use of air-filled cavities in microfluidic devices. Air filled cavities were seen to be stable over time scales of hours for PDMS channels and were stable during operation of the channels under pressure driven flow and electrokinetic flow. Flow properties were not significantly altered for either pressure flow or EO flow. An interesting mass transport effect was observed in the virtual wall channel when the fluid was heated. As mass transport occured, trapped air bubbles filled the main channel blocking flow eventually. This characteristic of mass transport has potential applications in microfluidics devices. A microvalve based on this mass transport effect was demonstrated. The valve has the advantages of simple design, simple fabrication, electronically programmable control, easy integration, no moving parts and zero dead volume. More applications of virtual wall devices are under study and will be reported in the future.

Although we have presented results with air-filled cavities paper, one can also apply the same methods to produce oil-filled cavities. Oil filled channels offer unique opportunities because their surface properties can be selected based on material. Virtual walls (air or oil) can be readily designed into microfluidic systems. Such devices warrant further study as a potentially useful tool in microfluidics.

ACKNOWLEDGMENT

The authors would like to thank Ruisheng Chang, Trang Bui, and the staff of the Integrated Nanosystems Research Facility at University of California, Irvine for their support in fabrication of the devices.

REFERENCES

[1] Duffy, D. C.; McDonald, J. C.; Schueller, O. J. A.; Whitesides, G. M. *Anal.Chem.* 1998, *70*, 4974-84.

[2] Grzybowski, B. A.; Haag, R.; Bowden, N.; Whitesides, G. M. *Anal. Chem.*1998, *70*, 4645-52.

[3] Barker, S. L. R.; Ross, D.; Tarlov, M. J.; Gaitan, M.; Locascio, L. E. *Anal.Chem.* 2000, *72*, 5925-9.

[4] Liu, Y.; Fanguy, J. C.; Bledsoe, J. M.; Henry, C. S. *Anal. Chem.* 2000, *72*, 5939-44.

[5] Linder, V.; Verpoorte, E.; Thormann, W.; de Rooji, N. F.; Sigrist, H. *Anal.Chem.* 2001, *73*, 4181-9.

[6] Shuwen H.; Xueqin R.; Mark B.; Christopher E. S.,| G. P. Li; Nancy A. *Anal. Chem.* 2002. 74, 4117-4123.

[7] Patankar, N. A. *Langmuir* 2003, *19*, 1249.

[8] Ashutosh S., Marianne J. C. and Karl F.B. IEEE-MEMS-Shastry-05

[9] Ou, Jia; Perot, Blair; Rothstein, Jonathan P. *Physics of Fluids*, 2004 Vol. 16, Issue 12, 4635-4643

[10] J. Kim and C.-J. Kim, in *IEEE Conference MEMS (Las Vegas, NV, 2002)*, p. 479.

[11] Javier Atencia and David J. Beebe *Nature* 437, 648-655

[12] Bin Z., Jeffrey S. M., David J. B., *Science* 9 February 2001:Vol. 291. no. 5506, pp. 1023 – 1026

[13] T. Onda, S. Shibuichi, N. Satoh and K. Tsuji, Super-water-repellent fractal surfaces, *Langmuir* vol.12, pp.2125-2127, 1996.

[14] C. Cottin-Bizonne, J. L. Barrat, L. Bocquet and E. Charlaix, Low-friction flows of liquid at nanopatterned interfaces, Nature Materials, vol.2, pp.237-240, 2003.